CSIRO PUBLISHING www.publish.csiro.au/journals/eg Copublished paper, please cite all three:
Exploration Geophysics, 2008, **39**, 52–59; *Butsuri-Tansa*, 2008, **61**, 52–59; *Mulli-Tamsa*, 2008, **11**, 52–59

A marine deep-towed DC resistivity survey in a methane hydrate area, Japan Sea

Tada-nori Goto[1,8], Takafumi Kasaya[1], Hideaki Machiyama[1], Ryo Takagi[1,7], Ryo Matsumoto[2], Yoshihisa Okuda[3], Mikio Satoh[3], Toshiki Watanabe[4], Nobukazu Seama[5], Hitoshi Mikada[6], Yoshinori Sanada[1], Masataka Kinoshita[1]

[1]Japan Agency for Marine-Earth Science and Technology (JAMSTEC) 2-15, Natsushima, Yokosuka, Kanagawa 237-0061, Japan.
[2]Department of Earth and Planetary Science, University of Tokyo, Hongo 7-3-1, Bunkyo-ku, Tokyo 113-0033, Japan.
[3]National Institute of Advanced Industrial Science and Technology (AIST), Geological Survey of Japan (GSJ), Institute for Geo-Resources and Environment (GREEN), AIST Tsukuba Central 7, Higashi 1-1-1, Tsukuba, Ibaraki 305-8567, Japan.
[4]Research Center for Seismology, Volcanology and Disaster Mitigation, Graduate School of Environmental Studies, Nagoya University, Furou-cho, Chikusa-ku, Nagoya 464-8602, Japan.
[5]Research Center for Inland Seas, Kobe University, 1-1 Rokkodai, Nada, Kobe 657-8501, Japan.
[6]Department of Civil and Earth Resources Engineering, Graduate School of Engineering, Kyoto University, Kyoto-Daigaku-Katsura, Nishikyo-ku, Kyoto 615-8540, Japan.
[7]Present address: Japan Drilling Co. Ltd., Shin-Horidome Bldg. 6F 2-4-3 Nihonbashi Horidome-cho, Chuo-ku, Tokyo 103-0012, Japan.
[8]Corresponding author. Email: tgoto@jamstec.go.jp

Abstract. We have developed a new deep-towed marine DC resistivity survey system. It was designed to detect the top boundary of the methane hydrate zone, which is not imaged well by seismic reflection surveys. Our system, with a transmitter and a 160-m-long tail with eight source electrodes and a receiver dipole, is towed from a research vessel near the seafloor. Numerical calculations show that our marine DC resistivity survey system can effectively image the top surface of the methane hydrate layer. A survey was carried out off Joetsu, in the Japan Sea, where outcrops of methane hydrate are observed. We successfully obtained DC resistivity data along a profile ~3.5 km long, and detected relatively high apparent resistivity values. Particularly in areas with methane hydrate exposure, anomalously high apparent resistivity was observed, and we interpret these high apparent resistivities to be due to the methane hydrate zone below the seafloor. Marine DC resistivity surveys will be a new tool to image sub-seafloor structures within methane hydrate zones.

Key words: DC resistivity survey, methane hydrate, deep-towed system, high apparent resistivity, piston coring.

Introduction

Methane hydrates (MHs) are naturally occurring solids consisting of methane and water at low temperature and high pressure. MH is mainly found in permafrost in polar regions, and in sedimentary layers along continental margins. A large amount of methane gas may be contained in the MH layer, so that MH is expected to be a new energy resource (e.g. Kvenvolden, 1993). On the other hand, MH will have a significant impact on global warming, because methane is one of the greenhouse gases.

Seismic reflectors approximately parallel to the seafloor are often identified below continental margins, and are often used to detect MH. They are called bottom simulating reflectors (BSRs). Since the polarity of the wavelet reflected from BSRs is opposite from that of seafloor reflections, BSRs are interpreted as a phase boundary between solid hydrate and free gas below the MH zone (Shipley et al., 1979). However, there are generally no clear seismic reflectors at the top boundary of the MH zone, and the upper bound of the MH zone has not been resolved well. In some cases, the existence of much gas hydrate has been inferred where no BSR was found (Paull et al., 2000).

In this paper, we introduce a new geophysical tool, sensitive to MH layers: a marine DC resistivity survey system. As summarised in Goldberg et al. (2000), the resistivity of a formation including massive MH may be as high as several tens of Ω.m, whereas sediments without MH typically have a resistivity of ~1 Ω.m. Thus, a resistivity survey has potential for imaging the MH zone. Recently, marine DC resistivity surveys have been carried out in shallow water areas (Lile et al., 1994; Inoue, 2005; Kwon et al., 2005; Allen and Merrick, 2007). For example, Kwon et al. (2005) conducted a DC resistivity survey with a floating cable and detected fault zones below a river bed. These recent studies show how effectively a marine DC resistivity survey can produce images of sub-seafloor structures. However, its applications to deep sea surveying have been rare. Von Herzen et al. (1996) carried out a pioneering DC resistivity survey on a hydrothermal mound by using a submersible, and estimated the resistivity of sulphides at shallow depths (<10 m). The water depth was ~3600 m.

Controlled-source electromagnetic (CSEM) soundings have been applied to detect MH zones below the deep seafloor. Yuan

 10.1071/EG08003 0812-3985/08/010052

and Edwards (2000) used a deep-towed CSEM source and two towed receivers, and found a relatively high resistivity layer related to MHs. Due to the limited number of their receivers, spatial and depth resolutions were quite limited in their study. Weitemeyer et al. (2006) used a deep-towed CSEM source and ocean-bottom receivers, and indicated lateral resistivity variation across a hydrate ridge. However, the horizontal resolution near the seafloor was limited because number of ocean-bottom receivers was limited. Therefore, we have adopted a deep-towed marine DC resistivity method, with multiple electrodes but without ocean-bottom receivers, for detecting MH zones. In this study, we first use numerical calculations to demonstrate how effectively a marine DC resistivity method images the top surface of MH layer. Then, we introduce a field test of our marine DC resistivity survey system.

System

Our new marine DC resistivity survey system is known as the 'MANTA' (MArine Navigated Towed Antennas), and is shown schematically in Figure 1. The MANTA is based on a conventional deep-towed (DT) system, originally developed by JAMSTEC (2007), with cameras, conductivity-temperature-depth sensors (CTD), an altimeter, and an AC transformer from 1400 VAC to 100 VAC. The DT system has no thrusters but is towed by a vessel, and is normally used to take seafloor visual images, water and rock samples. For a marine DC resistivity survey, a long tail is added to the DT system. This tail consists of eight cables with lengths from 56 to 157 m (Figure 1), four floats (glass spheres with diameter of 13 inches), and a sea anchor, tied into a bundle and adjusted to have neutral buoyancy. Eight raw copper wires 2 m in length are attached at the tips of the cables, and used for current electrodes (C1–7 and COM in Figure 1). The COM electrode and one other are selected to form a source dipole. For potential measurements, Ag-AgCl electrodes and two solid hoses are attached to the tail. Two Ag-AgCl electrodes are set at the rear of the DT frame, and hoses with length of 5 and 25 m are joined to each electrode as salt bridges. As a result, the voltage difference is measured with a 20 m dipole (P1–P2 in Figure 1). Acoustic transponders are attached to the DT frame and the end of the tail. These transponders can reply to an acoustic signal from the vessel with their own code, in a frequency band of 11–15 kHz. A super-short-baseline acoustic navigation system (SSBL), consisting of hull transducer arrays attached below the vessel, can detect the depths, horizontal directions and distances from the vessel to each of the transponders. As a result, the SSBL, the ship's GPS, the DT cameras and the altimeter make us possible for towing the MANTA's tail stably at ~5 m height above the seafloor. The maximum diving depth of the MANTA system is 6000 m.

A new transmitter for DC resistivity measurements is added on the frame of the DT system. The vessel supplies 3 kW of electric power, which is transformed to 100 VAC for input to the transmitter. The maximum output power of the transmitter is ~0.8 kW with maximum voltage of 72 V peak-to-peak and current of 44 A p-p. The waveform of the output current is normally sinusoidal, with a period of 4 s. The transmitter also has a digital recorder for the output voltage and current, temperature inside the pressure case, and the potential difference across the receiver dipole (P1–P2). The default sampling rate is 0.2 Hz. Finally, we obtain apparent resistivity values from respective source dipoles on the basis of the following equation:

$$\rho_a = 4\pi \frac{V}{I}\left(\frac{1}{r_1} - \frac{1}{r_2} - \frac{1}{r_3} + \frac{1}{r_4}\right), \quad (1)$$

where ρ_a denotes the apparent resistivity (Ω.m), I denotes the source current amplitude (A), V denotes the received voltage (V), r_1 to r_4 denotes distances (m) between electrodes; P1-Ci, P1-COM, P2-Ci and P2-COM, respectively. There are seven choices for current electrode, so Ci = C1 to C7.

The source dipole of our system is variable. One electrode of C1–C7 is used with COM to form the source dipole for one period of source current (4 s), and the choice of electrode is switched after each period. Therefore, our DC resistivity survey is based on the dipole-dipole method, but the length of the source dipole varies, and is different from the receiver dipole length. Pole-dipole DC resistivity sounding, as adopted by Inoue (2005), might be effective in our case if the metal cable between the DT and vessel (Figure 1) could be used for the current dipole. However, the cable length (8 km) limits the current amplitude because of heat production inside the cable, especially when

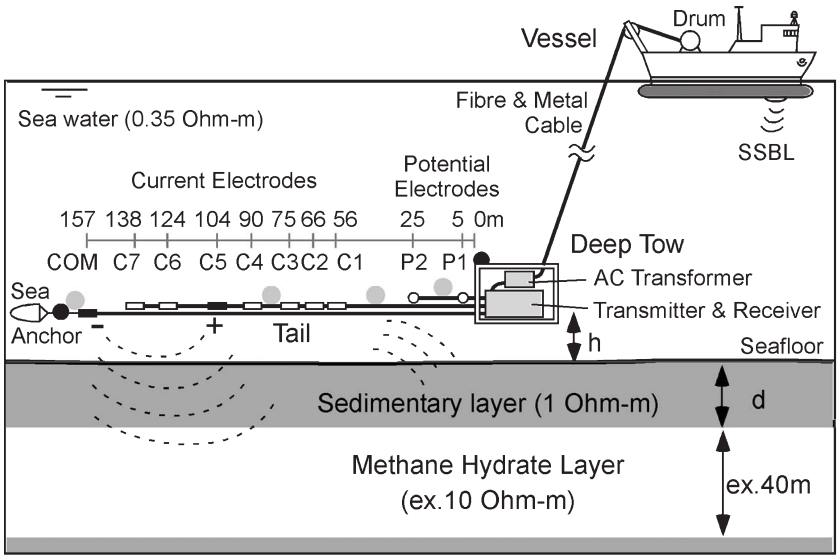

Fig. 1. Schematic diagram of the newly developed marine DC resistivity survey system, known as 'MANTA'. Dashed curves schematically indicate penetration of artificial electric field. C1–C7 & COM: source electrodes. P1, P2: receiver electrodes. Solid circles: acoustic transponders. Grey circles: 13-inch glass spheres for floats.

wound around the drum, which might melt the sheath. Therefore, we have adopted this quasi-dipole-dipole method. Qualitatively, the current electrode with lower number (e.g. C1) is closer to the receiver dipole and so has less sensitivity to the deep portion below the seafloor. In the other words, the C1-COM source dipole gives information on shallow resistivity structure, while the C7-COM gives deeper information. This prospect is demonstrated in the next section.

Feasibility tests

Apparent resistivities obtained by the MANTA system will reflect variations in depth to top, resistivity, and thickness of a MH layer, and also the height variation of the MANTA system from the seafloor. In this study, numerical calculations are carried out to check what kinds of factors affect the apparent resistivity, and to demonstrate how effectively the MANTA system might detect the MH layer. We assume a one-dimensional structure including a seawater layer with depth of 870 m and a sedimentary layer (Figure 1). The resistivity values of seawater and the sediment are 0.35 and 1 Ω.m, respectively. The assumed amplitude of source current is 32 A p-p. In order to estimate received voltage amplitude and apparent resistivity from equation (1), we modified a one-dimensional forward calculation code for DC resistivity sounding by Ushijima et al. (1987). The resistivity transform function in their original code (equation 3 in Ushijima et al., 1987) was for land, following Lagabrielle (1983; equation 2). In this study, we modified the function to one for water floor as introduced in equation 3 in Lagabrielle (1983). The linear filter method with coefficients for the Schlumberger array (Ghosh, 1971) was adopted to calculate electrical potential at the P1 and P2 electrodes. We also calculated predicted errors of the apparent resistivity. As the short-term fluctuation on the seafloor (during several seconds) is within 10 μV in general, we assumed the error in receiver voltage to be 10 μV, and calculate the resulting error in the apparent resistivity. In actual surveys, we normally adopt stacking and filtering of received signals to reduce the observed error, so that the predicted error in this feasibility study will be over-estimated.

First, numerical calculations with various MH layers are conducted. Here, the MANTA height (*h* in Figure 1) is fixed as 5 m. We assume the resistivity value of the massive MH layer as 10 Ω.m, based on a logging result from the Nankai Trough, off Tokai, Japan (Tezuka et al., 2002). We also assume the thickness of MH layer as 40 m, and vary the top depth (*d* in Figure 1). The calculated values are shown in Figure 2*a*, where the apparent resistivity curve varies greatly as the depth to the top of the MH layer is changed. It can also be seen that the various source dipoles in our DC marine resistivity survey have different sensitivity to the depth of the MH layer below the seafloor. For example, the source dipole with C1 and COM gives a relatively high apparent resistivity when the MH layer is located near the seafloor, but is less sensitive to the deeper MH layer as shown in Figure 2*a*. We have also checked the apparent resistivity variation if the resistivity or thickness of the MH layer is doubled (to 20 Ω.m or 80 m). The examples at $d = 0$, 40, and 100 m are shown as dashed and grey curves in Figure 2*a*. Although these variations increase the peak of the apparent resistivity curves, the shape of the curves is approximately the same. Therefore, we suggest that the distance from the nearest source electrode (e.g. C1, C2, . . .) to the receiver dipole represent an approximate sounding depth below the seafloor if the towed height (h) is kept as 5 m. We also suggest that the maximum sounding depth of the MANTA system is ∼100 m or more below the seafloor. By the way, the dashed and grey curves with the same top depth to the MH layer are similar each other. This suggests a trade-off between finding the resistivity and thickness of the MH layer by modelling using the observed apparent resistivity. The product of resistivity and thickness of MH layer may be determined well by our marine DC resistivity survey.

Next, we discuss how variation in the towed height of MANTA's tail affects the apparent resistivity estimation. Figure 2*b* indicates apparent resistivity curves obtained from various tail heights (*h* in Figure 1). Two sub-seafloor models with MH layer are used; shallow ($d = 0$ m) and deep ($d = 100$ m) MH with 10 Ω.m and 40 m thickness. The towed height variation affects the predicted apparent resistivity values, especially when an electrode close to the receiver dipole (e.g. C1) is used for the source dipole. As the tail becomes far from the seafloor, the seawater layer beneath the tail makes the apparent resistivity decrease. This effect is critical in the case of highly resistive seafloor ($d = 0$ m). It is suggested that sensitivity to the resistivity structure below the seafloor will decrease at large towed height. Comparing Figure 2*b* with 2*a*, we suggest that the height should be less than 10 m to obtain sub-seafloor information. The DT

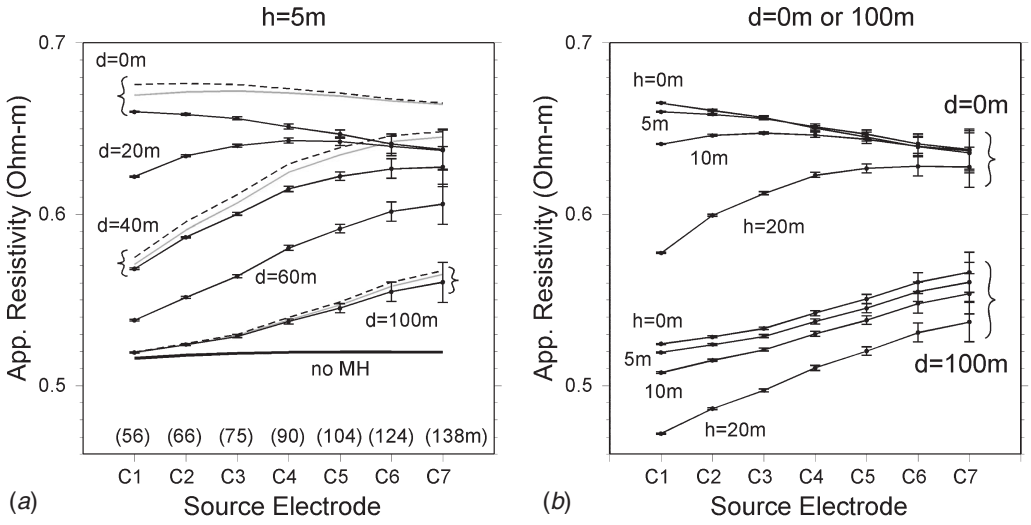

Fig. 2. Synthetic apparent resistivity curves obtained from numerical calculations. (*a*) Curves with various MH layer properties – thick curves: 1 Ω.m sediments, no MH; solid curves: various depths to the top of a MH layer (40 m thick and 10 Ω.m in resistivity); dashed curves: a more resistive MH layer (20 Ω.m); and grey curves: thicker MH layer (80 m). (*b*) Curves with various tail heights, over a MH layer (40 m thick and 10 Ω.m in resistivity).

camera and altimeter are important components when towing the DT frame at low clearance. Also, the difference between the acoustic transponders attached to the DT frame and the end of MANTA's tail, tracked by ship's SSBL in real time, enables us to monitor the height of MANTA's tail precisely and to tow it at a stable height. If the towed height is less than 10 m, a pseudosection (a spatial distribution of apparent resistivity obtained with various source dipoles) gives us a first-order image of the sub-seafloor structure. Quantitative interpretation of the structure requires an inversion process that takes into account the location of MANTA as well as the observed apparent resistivities.

Observations

Research cruise KY05–08, by JAMSTEC Research Vessel *Kaiyo* was conducted in August, 2005, for geological and geophysical investigation of MH in the Japan Sea. The Umitaka Spur, located off Joetsu, was selected as the survey area (Figure 3), where a gas hydrate field with highly active venting of methane had been recently found (Matsumoto et al., 2005; Tomaru et al., 2007). Camera observations with the DT system (without the tail) during the KY05–08 cruise, showed grey or shiny coloured seafloor and steep cliffs with several metre gaps. These anomalous seafloor features were found in two narrow areas with widths of ~100 m (MH1 and MH2 in Figure 3). In addition, massive or melted methane hydrate samples were obtained at shallow depth (<3 m) by piston coring during both the UT04 (Matsumoto et al., 2005) and KY05–08 cruises (Figure 3). These camera and core sampling results suggest the MH exposure in the areas MH1 and MH2.

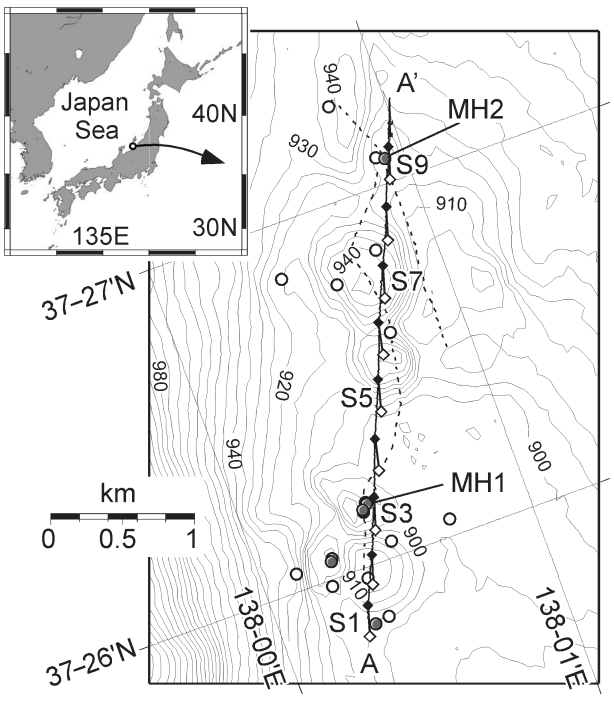

Fig. 3. Bathymetric map of the Umitaka Spur in the Japan Sea. A solid line indicates the track of the MANTA system. Solid and open diamonds indicate simultaneous horizontal position of the DT and the end of the resistivity system tail every 10 min, respectively. S1–S9 denote representative DT and tail positions. Dash lines are tracks of camera observations on the KY05–08 cruise, showing that the seafloor at areas MH1 and MH2 had anomalous grey or shiny colour. Grey and open circles indicate the location of piston coring with and without MH samples, respectively, collected in both the UT04 (Matsumoto et al., 2005) and the KY05–08 cruises.

The newly developed MANTA system was deployed from R/V *Kaiyo* (Figure 4) and operated on the Umitaka Spur to test whether the marine DC resistivity survey could detect MHs effectively, as shown in Figure 2. Along the profile A-A', with length of ~3.5 km (Figure 3), The MANTA system was towed at a speed of ~1 km, and the MANTA's tail height was kept within 20 m along the most part of profile. Simultaneous camera observation was carried out. The location and depth of the DT was tracked by the ship's SSBL in real time (Figure 6). The end of the tail, trailing the DT, was also tracked by SSBL. The tail cannot respond to abrupt depth changes of the DT, but takes a smooth 'shortcut' route along the DT track. For 90 min, the MANTA system continued to transmit current and record potential differences near the seafloor. An example of raw time-series data is shown in Figure 5*a*. Because the distance from

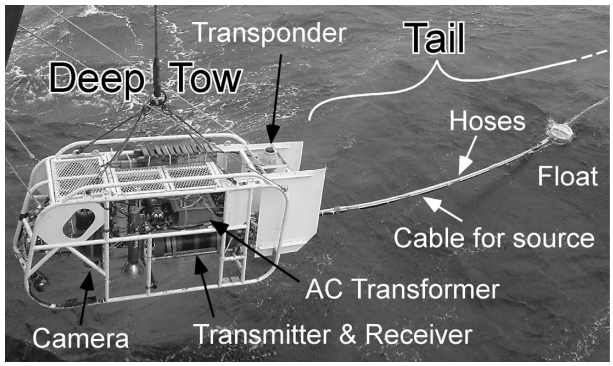

Fig. 4. Deployment of the MANTA system. The DT frame height is ~2 m.

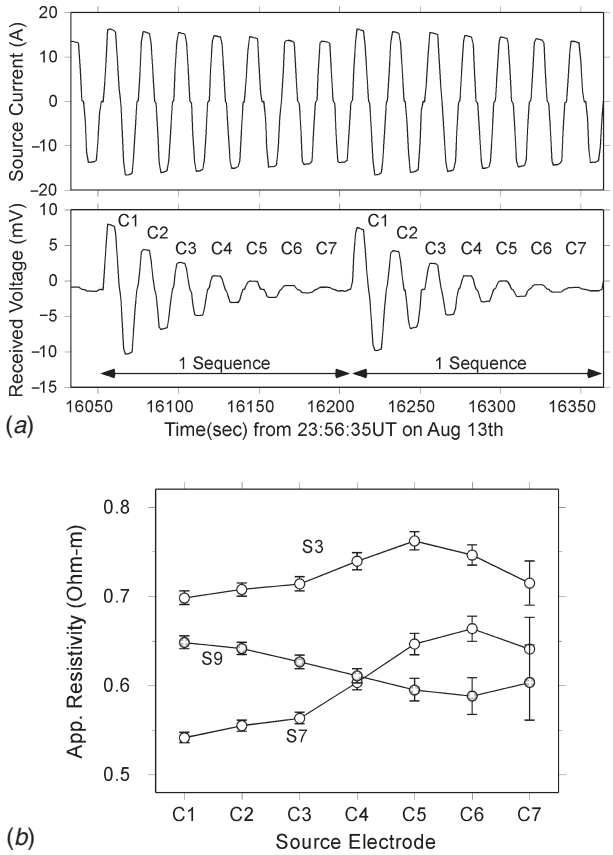

Fig. 5. (*a*) An example of raw time-series data of source current and received voltage difference. These data were obtained near S3. C1–C7: source electrodes. (*b*) Examples of observed apparent resistivity at locations S3, S7, and S9.

an active electrode of the source dipole to the receiver dipole is changed every 4 s, as described above, the amplitude of the potential difference also changed every 4 s. Note that the source amplitude also changes slightly. This is because the transmitter was driven with a constant voltage of 72 V p-p, and the total cable length (i.e. total resistance) of the source dipole changes.

Apparent resistivity values from the marine DC resistivity survey are estimated about every 50 m horizontally, with seven different source dipoles. First, a time segment was defined as including consecutive signals from the seven source dipoles (Figure 5*a*). Every three segments (∼90 s) of the raw time series data were stacked, corresponding horizontal sampling rate of ∼50 m with 1 km towing speed. The ratio between the stacked source current and potential amplitude was estimated for each of the respective source dipoles, using the least-squares method. No filtering method was applied here. Then, we applied calibration factors to the observed ratios to avoid unwanted effects of the main metallic cable and the DT frame on the potential measurement. For system calibration, the MANTA system towed at a depth of 400 m for 15 min, far from the sea surface and seafloor, so that the apparent resistivity obtained should be same as the seawater resistivity. The resistivity of the seawater was measured simultaneously with the CTD sensor, so that the calibration factors for each source dipoles could be estimated. The actual CTD resistivity, raw apparent resistivities, and the calibration factors are summarised in Table 1. Finally, observed apparent resistivity near the seafloor was estimated using equation (1).

Results

Observed apparent resistivities are estimated with high accuracy, and indicate relatively high values. Representative curves at locations S3, S7, and S9 (Figures 3 and 5*b*), where both height of the DT and the tail were less than 10 m, are shown in Figure 5*b*. The estimation errors are less than 0.01 Ω.m when the electrodes C1 to C4 are used as source electrodes, while larger errors of 0.01–0.04 Ω.m may occur when electrodes C6 or C7 is used. The larger errors are due to the relatively shorter source dipole length and the longer distance from the source to the potential dipole. Taking into consideration the observed errors, the apparent resistivity values are higher than 0.5 Ω.m. The CTD sensor gives us the uniform resistivity of seawater as ∼0.35 Ω.m with perturbations less than 0.1%, so that the observed apparent resistivity values at these representative locations are higher than the seawater resistivity. We also estimated errors in the depths of the DT and tail. Around S4, with stable towing for 90 s, the standard error in the CTD depth was ∼0.03 m. Also, the standard error of the depth of tail end, estimated by SSBL, was ∼0.5 m. On the basis of Figure 2*b*, a change of tail height with 0.5 m would lead to apparent resistivity changes of 0.01–0.03 Ω.m. Therefore, even including the contribution of towed depth errors, the observed apparent resistivity is definitely higher than seawater resistivity.

The spatial distribution of apparent resistivity indicates that high values are recognised below part of the profile, and very high values are recognised in two narrow areas. The pseudosection of apparent resistivity is shown in Figure 6, in which the locations of DT and one of source electrodes are taken as the horizontal and vertical axes, respectively. Here, the apparent resistivity values obtained at a specific location (e.g. S3) are plotted vertically below the DT position. An area between S7 and S9 shows high apparent resistivity (>0.6 Ω.m). The apparent resistivity for source electrodes C4 to C7, relatively far from the receiver dipole, is much higher than the resistivity for source electrodes C1 to C3. In addition, very high apparent resistivity values with source electrodes of C1 to C3 are also recognised below two narrow areas; MH1 and MH2. On the other hand, low apparent resistivity values (<0.5 Ω.m) are obtained in areas around S1 and between S4 and S6. The height of DT and tail in these areas was 20 m or more, so the low apparent resistivity values mainly reflect seawater resistivity and include less information on the sub-seafloor structure.

Discussion

The observed high apparent resistivity (Figure 5*b*) cannot be explained by normal sediments below the seafloor. As shown in Figure 2*a*, the apparent resistivity on the sub-seafloor structure without MH is less than 0.6 Ω.m. If a high resistivity layer (10 Ω.m) with thickness of 40 m were located with its top depth 20–40 m below the seafloor, the apparent resistivity obtained would be greater than 0.6 Ω.m (Figure 2). Therefore, shallow resistive layers below the seafloor can explain the high apparent resistivity observed, greater than 0.6 Ω.m.

The high apparent resistivity possibly corresponds to the MH distribution on the seafloor. In the pseudosection (Figure 6), very high apparent resistivity values are observed with the source electrodes C1 to C3 below the areas MH1 and MH2. The source dipoles with closer electrodes such as C1 give us information on the shallow sub-seafloor structure if the towed height is low, so that such high apparent resistivity values should reflect shallow resistive zones. As already described, the anomalously coloured seafloor images (Figure 3) and piston coring samples of massive MH (Figure 7) were obtained in the MH1 and MH2 areas. This coincidence with the pseudosection, the camera images, and the core samples suggest that the very high apparent resistivity is related to MH near the seafloor. In the areas between S7 and S9, high apparent resistivity values (>0.6 Ω.m) are also obtained with the source electrodes of C4 to C7 in an area between S7 and S9. Because the towed height is less than 10 m in this area, these source dipoles present deeper resistivity information as suggested earlier. We interpret such high apparent resistivities to be related to an unexposed deep MH zone.

The estimation of the depth of the MH layer is not yet straightforward. As described earlier, an approximate sounding depth below the seafloor is inferred from the distance between a source electrode and the receiver dipole, if the towed height is

Table 1. Seawater resistivity measured by CTD during calibration, raw apparent resistivities measured by the MANTA system during calibration, and the calibration factors.

Calibration (02:20–02:40 UT on Aug 13)

CTD resistivity (Ω.m)	0.3415 in average (max = 0.3417; min = 0.3413)						
Source dipole	C1-COM	C2-COM	C3-COM	C4-COM	C5-COM	C6-COM	C7-COM
Raw app. res. (Ω.m)	0.3261	0.3324	0.3361	0.3004	0.3030	0.3101	0.3176
App. res. error (Ω.m)	0.0032	0.0032	0.0036	0.0037	0.0044	0.0082	0.0201
Calibration factors	1.0472	1.0273	1.0161	1.1367	1.1271	1.1014	1.0752
Calibration error (%)	0.9789	0.9626	1.0679	1.2389	1.4665	2.6347	6.3430

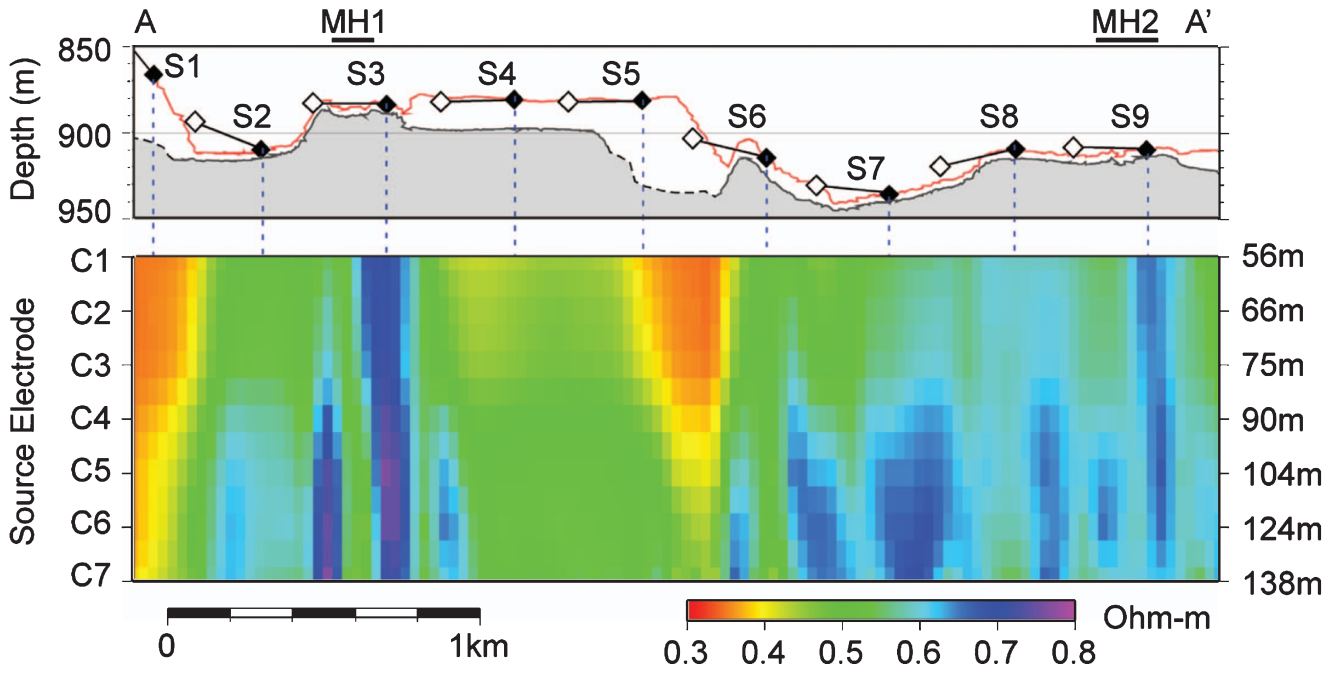

Fig. 6. Pseudosection of apparent resistivity along the profile A-A' (Figure 3). The vertical axis is not to scale, but the electrode numbers for the source dipoles are used to represent the distance between the electrode and DT, in turn representing approximate sounding depth below the seafloor if the MANTA's towed height is low. A cross-section of the bathymetry is also shown at the top. The bathymetry is derived from the sum of CTD depth and height by altimeter (solid lines), or the ship's multi narrow beam echo sounder (dashed lines). Solid and open diamonds indicate simultaneous locations of the DT and the end of the resistivity system tail every 10 min, and solid lines connecting diamonds represent the MANTA resistivity system tail. A red line indicates the DT track based on the CTD depth and the horizontal position by SSBL. Locations S1–S9, MH1, and MH2 are the same as in Figure 3.

low. The high apparent resistivity with source electrodes of C4 to C7 (at the area between S7 and S9) implies that the top of MH layer is probably deeper than several tens of metres below the seafloor. On the other hand, the very high apparent resistivity in the areas MH1 and MH2 with source electrode of C1 implies that the top of the MH layer will be shallower than several tens of metres. Therefore, a heterogeneous distribution of the depth to the top of the MH layer is inferred from our qualitative interpretation. However, for further discussion, quantitative estimation of the depth extent of the MH layer is required. One-dimensional or two-dimensional inversion procedures are necessary for the deep-tow marine DC resistivity survey, and are now under development. The topographic effect and the towed-height effect should be also carefully dealt in this development.

Conclusions

In order to detect MH distributions, especially the top boundary, we have developed a new marine DC resistivity survey system (MANTA), consisting of a deep-towed system, a transmitter and a 160 m long tail with source electrodes and a receiver

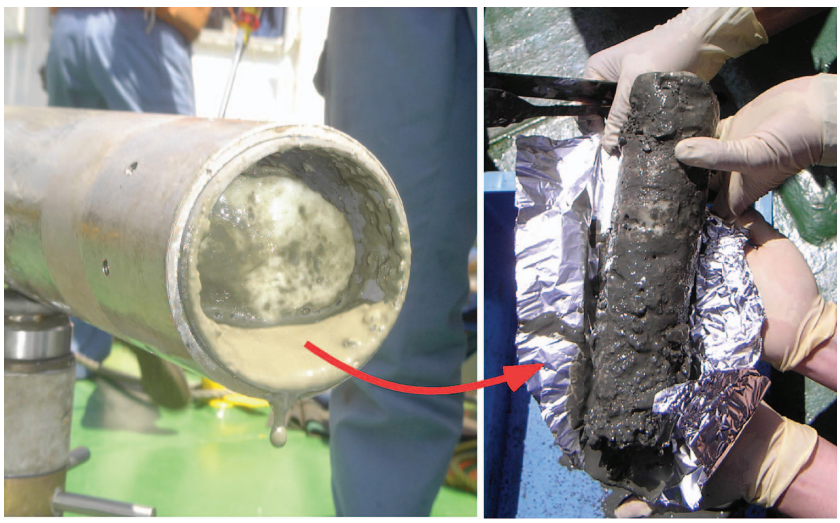

Fig. 7. A massive methane hydrate sample collected by piston coring in the area MH1 (Figure 3) in the KY05–08 cruise (Figure 3). Left: MH revealed after removing the core catcher. Right: MH sample pulled out from the inner tube. Although the sample is covered by mud, the whole of this sample is massive hydrate, white in colour.

dipole. The MANTA system can dive down to 6000 m water depth, and can be towed at 5 m clearance above the seafloor. The feasibility of the MANTA system has been discussed on the basis of numerical studies.

We have carried out field tests off Joetsu, in the Japan Sea, over recently recognised MH-exposed areas. Apparent resistivity is estimated with high accuracy, and indicates relatively high values, implying the existence of resistive material below the seafloor. Around the areas with methane hydrate exposure, anomalously high apparent resistivity is observed with short source-receiver separations, so that we interpret these high apparent resistivities to be due to the MH zone below the seafloor. On the basis of a pseudosection, we infer a heterogeneous distribution of the depth to the top of the MH layer. Although qualitative imaging has been achieved, inversion codes that take into account the MANTA's electrode locations and the bathymetry are necessary for further discussion and estimation of the precise depth and resistivity estimation of the MH zone.

As a result of the field test of the MANTA system, we can image the sub-seafloor structure continuously with horizontal resolution of several tens of metres. The maximum sounding depth is ~100 m. The towed speed was 1 kn normally, so that we can 'scan' the resistivity structure along a total profile length of ~40 km/day. Therefore, we propose that our MANTA system will be useful for two-dimensional or three-dimensional imaging with parallel profiles, to detect MH zones in a wide area.

Acknowledgments

We are grateful for extensive support by the captain and ship's crews on R/V *Kaiyo*, and by marine technicians and the Research Support Department in JAMSTEC. We thank Dr G. Snyder, H. Tomaru, and H. Lu for helping on the KY05–08 cruise. We also thank students at University of Tokyo, Kobe University, Chiba University, and Kyoto University. The forward code for DC resistivity calculations was originally developed by Dr K. Ushijima, Dr H. Mizunaga and Dr A. Kato of Kyushi University. Helpful comments about methane hydrate exploration were given by JOGMEC, especially Dr. T. Saeki. The manuscript was greatly improved by reviewers and editors. This project is partially supported by the Ministry of Education, Culture, Sports, Science and Technology, Grant-in-Aid for Scientific Research, 16360449, 2006.

References

Allen, D., and Merrick, N., 2007, Robust 1D inversion of large towed geo-electric array datasets used for hydrogeological studies: *Exploration Geophysics* **38**, 50–59. doi: 10.1071/EG07003

Ghosh, D. P., 1971, Inverse filter coefficients for the computation of apparent resistivity standard curves for a horizontally stratified earth: *Geophysical Prospecting* **19**, 769–775. doi: 10.1111/j.1365-2478.1971.tb00915.x

Goldberg, D., Collett, T. S., and Hyndman, R. D., 2000, Ground truth: in-situ properties of hydrate, in Max, M.D., ed., *Natural Gas Hydrate in Oceanic and Permafrost Environments*: Dordrecht, Kluwer Academic Publishers, 295–310.

Inoue, M., 2005, Development and case studies of the new submarine electric sounding system: *Geophysical Exploration* **58**, 241–250.

JAMSTEC 2007, JAMSTEC official Web site, "DEEP TOW, Research Vessels and Vehicles", <http://www.jamstec.go.jp/e/about/equipment/ships/deepto.html> (accessed December 10, 2007).

Kvenvolden, K. A., 1993, Gas hydrates-geological perspective and global change: *Reviews of Geophysics* **31**, 173–187. doi: 10.1029/93RG00268

Kwon, H.-S., Kim, J.-H., Ahn, H.-Y., Yoon, J.-S., Kim, K.-S., Jung, C.-K., Lee, S.-B., and Uchida, T., 2005, Delineation of a fault zone beneath a river bed by a DC resistivity survey using a floating streamer cable: *Exploration Geophysics* **36**, 50–58. doi: 10.1071/EG05050

Lagabrielle, R., 1983, The effect of water on direct current resistivity measurement from the sea, river or lake floor: *Geoexploration* **21**, 165–170. doi: 10.1016/0016-7142(83)90006-6

Lile, O. B., Backe, K. R., Elvebakk, H., and Buan, J. E., 1994, Resistivity measurements on the sea bottom to map fracture zones in the bedrock underneath sediments: *Geophysical Prospecting* **42**, 813–824. doi: 10.1111/j.1365-2478.1994.tb00242.x

Matsumoto, R., Okuda, Y., Aoyama, C., Hiruta, A., Ishida, Y., et al., 2005, Methane plumes over a marine gas hydrate system in the eastern margin of Japan Sea: a possible mechanism for the transportation of subsurface methane to shallow waters: *Proceedings of the 5th International Conference on Gas Hydrates, Trondheim, Norway*, **3**, 749–754.

Paull, C. K., Matsumoto, R., Wallace, P. J., and Dillon, W. P., 2000, *Proceedings of the Ocean Drilling Program*, Scientific Results, **164**.

Shipley, T. H., Houston, M. H., Buffler, R. T., Shaub, F. J., McMillen, K. J., Ladd, J. W., and Worzel, J. L., 1979, Seismic evidence for widespread possible gas hydrate horizons on continental slopes and rises: *AAPG Bulletin* **63**, 2204–2213.

Tezuka, K., Miyairi, M., Uchida, T., and Akihisa, K., 2002, Well log analysis for methane hydrate bearing formation: *Geophysical Exploration* **55**, 413–424.

Tomaru, H., Lu, Z., Snyder, G. T., Fehn, U., Hiruta, A., and Matsumoto, R., 2007, Origin and flow of pore waters in an actively venting gas hydrate field near Sado Island, Japan Sea: interpretation of halogen and 129I distributions: *Chemical Geology* **236**, 350–366. doi: 10.1016/j.chemgeo.2006.10.008

Ushijima, K., Mizunaga, H., and Kato, A., 1987, Interpretation of Geoelectric Sounding Data by Personal Computer: *Geophysical Exploration (Butsuri-Tansa)* **40**, 423–435.

Von Herzen, R. P., Kirklin, J., and Becker, K., 1996, Geoelectrical measurements at the TAG hydrothermal mound: *Geophysical Research Letters* **23**, 3451–3454. doi: 10.1029/96GL02077

Weitemeyer, K. A., Constable, S. C., Key, K. W., and Behrens, J. P., 2006, First results from a marine controlled-source electromagnetic survey to detect gas hydrates offshore Oregon: *Geophysical Research Letters* **33**, L03304. doi: 10.1029/2005GL024896

Yuan, J., and Edwards, R. N., 2000, The assessment of marine gas hydrate through electrical remote sounding: hydrate without a BSR?: *Geophysical Research Letters* **27**, 2397–2400. doi: 10.1029/2000GL011585

Manuscript received 31 October 2007; accepted 14 December 2007.

日本海メタンハイドレート地域における海底曳航式電気探査調査

後藤忠徳[1]・笠谷貴史[1]・町山栄章[1]・高木　亮[1,7]・松本　良[2]・奥田義久[3]・佐藤幹夫[3]・
渡辺俊樹[4]・島　伸和[5]・三ヶ田　均[6]・真田佳典[1]・木下正高[1]

要　旨：　地震波反射法では不明瞭なメタンハイドレート帯の上面を検出するために，我々は新しい深海曳航式海底電気探査システムを開発した。本システムは 8 つの送信電極と 1 組の受信電極からなる 160m 長のケーブルと人工電流送信機を有しており，調査船を用いて海底付近を曳航することができる。数値計算の結果，この海底電気探査システムはメタンハイドレート帯の上面をイメージできることが分かったため，日本海において実海域試験を行った。調査海域の海底にはメタンハイドレートが露出している。実海域試験では約 3.5km の測線において海底電気探査が実施された。その結果，相対的に高い見掛比抵抗値を得ることに成功した。特にメタンハイドレート露出域では非常に高い見掛比抵抗値異常が観測された。このことから高い見掛比抵抗値はメタンハイドレート帯に対応するものであると解釈でき，海底電気探査はメタンハイドレート帯をイメージする新たなツールであると言える。

キーワード：電気探査，メタンハイドレート，深海曳航式，高見掛比抵抗，ピストンコアリング

동해의 메탄 하이드레이트 매장 지역에서의 해양 심부 견인 전기비저항 탐사

Tada-nori Goto[1], Takafumi Kasaya[1], Hideaki Machiyama[1], Ryo Takagi[1,7], Ryo Matsumoto[2], Yoshihisa Okuda[3], Mikio Satoh[3], Toshiki Watanabe[4], Nobukazu Seama[5], Hitoshi Mikada[6], Yoshinori Sanada[1], and Masataka Kinoshita[1]

요 약：　해양 심부 견인 전기비저항 탐사 방법이 새로이 개발되었다. 이 방법은 탄성파 반사법 탐사에서 잘 영상화되지 않던 메탄 하이드레이트의 상부 경계를 찾아내기 위해 고안되었다. 이 장비는 하나의 송신기와 8개의 송신 전극들 및 한 개의 수신쌍극자를 갖는 160 m 연장의 긴 꼬리가 연구용 탐사선에 연결 되어 해저면 근처에서 끌리도록 만들어져 있다. 수치모형실험은 고안된 해양 전기비저항 탐사 방법이 메탄 하이드레이트 층의 상부를 효과적으로 잘 영상화함을 보여주었다. 실제 탐사는 메탄 하이드레이트가 노두로 관찰된 동해에 속해 있는 Joetsu의 먼바다에서 수행되었다. 대략 3.5 km에 달하는 탐사측선에 대하여 전기비저항 자료가 성공적으로 얻어 졌으며 상대적으로 높은 겉보기비저항 값들이 감지되었다. 특별히 메탄 하이드레이트가 들어나 있는 지역에서는 이상적으로 높은 겉보기비저항 값이 관측되었으며, 우리는 이 고겉보기비저항 값이 해저면 밑의 메탄 하이드레이트 지역에 의한 것으로 해석 하였다. 해양 전기비저항 탐사는 메탄 하이드레이트가 매장되어 있는 지역에서 해저면 하부를 잘 영상화 할 수 있는 새로운 도구가 될 것이다.

주요어：전기비저항탐사, 메탄 하이드레이트, 심부 견인 장치, 고겉보기비저항, 피스톤 코어링

1 海洋研究開発機構
〒237-0061　神奈川県横須賀市夏島町 2-15
2 東京大学大学院 理学系研究科 地球惑星科学専攻
3 産業技術総合研究所 地圏資源環境研究部門
4 名古屋大学大学院 環境学研究科附属地震火山・防災研究センター
5 神戸大学 内海域環境教育研究センター
6 京都大学大学院 工学研究科 社会基盤工学専攻
7 現在：日本海洋掘削（株）

1 일본 해양연구개발기구
2 동경대학 지구 및 천문학과
3 일본 산업기술종합연구소 지구자원환경연구부문
4 나고야 대학, 환경대학원, 지진, 화산 및 재난 방재 연구 센터
5 고베 대학, 내륙해 연구 센터
6 쿄토 대학, 공학연구과 사회기반공학전공
7 현재: 일본 해양굴착 (주)